Effects of lattice distortion and Jahn - Teller coupling on the magnetoresistance of $La_{0.7}Ca_{0.3}MnO_3$ and $La_{0.5}Ca_{0.5}CoO_3$ epitaxial films

1997 J. Phys.: Condens. Matter 9 3713

(http://iopscience.iop.org/0953-8984/9/18/010)

J. Phys.: Condens. Matter **9** (1997) 3713–3721. Printed in the UK PII: S0953-8984(97)78574-6

Effects of lattice distortion and Jahn–Teller coupling on the magnetoresistance of $La_{0.7}Ca_{0.3}MnO_3$ and $La_{0.5}Ca_{0.5}CoO_3$ epitaxial films

N-C Yeh†, R P Vasquez‡, D A Beam†, C-C Fu†, J Huynh† and G Beach†‡

† Department of Physics, California Institute of Technology, Pasadena, CA 91125, USA
‡ Center for Space Microelectronics Technology, Jet Propulsion Laboratory, California Institute of Technology, Pasadena, CA 91109, USA

Received 10 October 1996

Abstract. Studies of $La_{0.7}Ca_{0.3}MnO_3$ epitaxial films on substrates with a range of lattice constants reveal two dominant contributions to the occurrence of colossal negative magnetoresistance (CMR) in these manganites: at high temperatures ($T \rightarrow T_C$, T_C being the Curie temperature), the magnetotransport properties are predominantly determined by the conduction of lattice polarons, while at low temperatures ($T \ll T_C$), the residual negative magnetoresistance is correlated with the substrate-induced lattice distortion which incurs excess magnetic domain wall scattering. The importance of lattice polaron conduction associated with the presence of Jahn–Teller coupling in the manganites is further verified by comparing the manganites with epitaxial films of another ferromagnetic perovskite, $La_{0.5}Ca_{0.5}CoO_3$. Regardless of the differences in the substrate-induced lattice distortion, the cobaltite films exhibit much smaller negative magnetoresistance, which may be attributed to the absence of Jahn–Teller coupling and the high electron mobility that prevents the formation of lattice polarons. We therefore suggest that lattice polaron conduction associated with the Jahn–Teller coupling is essential for the occurrence of CMR, and that lattice distortion further enhances the CMR effects in the manganites.

1. Introduction

Recent findings of colossal negative magnetoresistance (CMR) in the perovskite manganites $Ln_{1-x}A_xMnO_{3-\delta}$ (Ln: trivalent rare-earth ions; A: divalent alkaline-earth ions) have spurred on intense research on understanding the origin and providing further improvement of the magnetoresistive effects [1–8]. It has been known for decades that the magnetic phases and electronic properties of these manganites vary with the doping level (x) [9–13]. Upon increasing x, the concentration of Mn^{4+} increases, giving rise to a mixture of Mn^{3+} and Mn^{4+} which initially yields canted spin configurations [11–13] and then forms metallic bonding and ferromagnetism for doping levels in the range $0.2 \leqslant x \leqslant 0.4$ [9–13]. The occurrence of ferromagnetism had been attributed to the double-exchange interaction between Mn^{3+} and Mn^{4+} ions [9–13]. However, further theoretical investigations revealed that the double exchange alone cannot quantitatively account for the observed CMR effect, and that the strong electron–phonon interaction arising from the Jahn–Teller splitting may be important [2]. The suggested relevance of the lattice effects on the conductivity and magnetism of these manganites is supported by increasing experimental evidence: a strong correlation between the thickness of the epitaxial films and the corresponding

0953-8984/97/183713+09$19.50

magnetoresistance has been revealed in the $La_{0.7}Sr_{0.3}MnO_3$ system [3]; decreasing Curie temperatures and increasing CMR effects in $La_{0.7-x}Ln'_xCa_{0.3}MnO_3$ ($Ln' = Pr$, Y; $0 \leqslant x \leqslant 0.7$) polycrystalline materials with decreasing lanthanide average ionic size have been demonstrated via the substitution of the smaller ions of Pr and Y for the La [4]; studies of $La_{0.6}Pb_{0.4}MnO_3$ and $Nd_{0.6}(Sr_{0.7}Pb_{0.3})_{0.4}MnO_3$ single crystals have illustrated magnetoresistance much smaller than that in the polycrystalline samples [5]; a significant reduction of the magnetoresistance has been observed in $Nd_{0.5}Sr_{0.36}Pb_{0.14}MnO_3$ single crystals under a hydrostatic pressure of 10.7 kbar [6]; and a large magnetovolume effect [7] and a giant oxygen isotope effect [8] have been found in polycrystalline samples of $La_{1-x}Ca_xMnO_3$.

To seek further understanding of the role of the lattice distortion and the Jahn–Teller effect as regards the occurrence of CMR in the manganites, particularly manganites in the thin-film form which are potentially important for the development of magnetic devices, we report in this work experimental investigations of the transport and magnetic properties of $La_{0.7}Ca_{0.3}MnO_3$ and $La_{0.5}Ca_{0.5}CoO_3$ epitaxial films on various perovskite substrates. The substrates selected include single-crystalline (001) $LaAlO_3$ (LAO), $SrTiO_3$ (STO), and $YAlO_3$ (YAO). As shown in table 1, these substrates are chosen to provide a range of lattice constants, which allows studies of the effects of tensile and compressive stress of the films. By maintaining the same chemical composition, oxygen annealing condition, and film thickness for all samples, we can investigate the net effect of substrate-induced lattice distortion on the transport and magnetic properties. To investigate the relevance of the Jahn–Teller coupling, we consider the cobaltites $La_{1-y}Ca_yCoO_3$ which are known to be highly conductive ferromagnets at doping levels of $0.4 \leqslant y \leqslant 0.6$ [12, 14]. In these cobaltites, the Co^{3+} and Co^{4+} ions are known to exist in the form of both high-spin and low-spin states [12], with either entirely empty or half-filled e_g orbitals which are responsible for the high electrical conductivity and ferromagnetism [15]. However, neither the empty nor the half-filled e_g orbitals in the cobaltites yield any Jahn–Teller effect. The high mobility of the conduction electrons together with the absence of the Jahn–Teller effect render the electron–phonon interaction in the cobaltites far less significant than that in the manganites.

2. Experimental details

The $La_{0.7}Ca_{0.3}MnO_3$ (LCMO) and $La_{0.5}Ca_{0.5}CoO_3$ (LCCO) epitaxial films are grown by pulsed laser deposition using stoichiometric targets of $La_{0.7}Ca_{0.3}MnO_3$ and $La_{0.5}Ca_{0.5}CoO_3$. The films are grown in 100 mTorr of oxygen with the substrate temperature at 700 °C, and subsequently annealed at 900 °C in 1 atm oxygen for two hours. The oxygen concentration is believed to be stoichiometric because longer annealing times do not yield further increase of the Curie temperature T_C, and the T_C-values for all LCMO ($T_C = 260 \pm 10$ K) and LCCO ($T_C = 180 \pm 5$ K) films on different substrates are consistent with those for the bulk material, as determined from the low-frequency magnetic susceptibility measurements made using the standard lock-in technique. The thickness of all samples is 200 ± 10 nm, and the lattice constants a, b, and c ($\boldsymbol{c} \perp$ sample surface) as well as the epitaxy of the films are determined using high-resolution x-ray diffraction and x-ray rocking curves. The results are tabulated in table 1. The chemical properties of these samples were further characterized with x-ray photoelectron spectroscopy (XPS) [16]. The results indicate that no interdiffusion takes place between the substrate material and the film except for in the LCCO/STO case. Furthermore, no density of states at the Fermi level was observed for the manganites [16], consistent with the semiconducting nature of these samples at room temperature. In contrast, a high density of states at the Fermi level is observed for the

cobaltites [16], in agreement with their metallic nature.

To correlate the physical properties of both the manganites and cobaltites with the structural studies of the lattice distortion, various experiments have been performed, including measurements of the resistivity, magnetization, and optical conductivity [17], as well as surface topography and tunnelling spectroscopy using a low-temperature scanning tunnelling microscope [18]. In this work we focus on the transport and magnetic properties, and then compare these results with the optical and STM studies. The dimensions of the samples are 2 mm × 2 mm × 200 nm, and the standard four-probe measurements are performed. The resistivity is measured in a magnetic field varying from 0 to 6 T, and the anisotropic magnetoresistance is studied by varying the orientation of the magnetic field from 0 to 90° relative to the sample surface. The applied current is always transverse to the external field. The magnetic field and temperature dependence of the resistivity is found to be comparable for all orientations. The magnetization measurements are performed using a SQUID magnetometer made by Quantum Design, with the applied field parallel to the sample surface.

Table 1. The lattice constants, lattice relaxation, and mismatch lattice strain determined from x-ray diffraction for $La_{0.7}Ca_{0.3}MnO_3$ (LCMO) and $La_{0.5}Ca_{0.5}CoO_3$ (LCCO) epitaxial films on $LaAlO_3$ (LAO), $YAlO_3$ (YAO) and $SrTiO_3$ (STO) substrates at 300 K. For comparison, the lattice constants (in Å) are for bulk LCMO: $a/\sqrt{2} = 3.840, b/\sqrt{2} = 3.890, c/2 = 3.860$; for LCCO: $a = b = c = 3.797$ [22]; for LAO: $a = b = c = 3.792$; for YAO: $a/\sqrt{2} = 3.662, b/\sqrt{2} = 3.768, c/2 = 3.685$; and for STO: $a = b = c = 3.905$.

	Lattice constant (Å)			Lattice relaxation (%)		Lattice strain (%)		
Compound	$a/\sqrt{2}$	$b/\sqrt{2}$	$c/2$	$\Delta a_s/a_s$	$\Delta b_s/b_s$	$\Delta a_0/a_0$	$\Delta b_0/b_0$	$\Delta c_0/c_0$
LCMO/LAO	3.842	3.854	3.921	1.32	1.64	0.05	−0.93	1.58
LCMO/YAO	3.862	3.886	3.899	4.80	3.08	0.57	−0.10	1.01
LCMO/STO	3.881	3.927	3.845	0.62	0.56	1.07	0.95	−0.39
LCCO/LAO	3.790	3.790	3.793	−0.05	−0.05	−0.18	−0.18	−0.11
LCCO/YAO	3.828	3.823	3.777	4.59	1.41	0.82	0.68	−0.53

3. Results, analyses, and discussion

The lattice distortion induced by the substrates yields two relevant effects. One is the lattice strain, defined as $\Delta a_0/a_0$, where a_0 is the lattice constant of the bulk perovskite, and Δa_0 is the difference between the lattice constant of the film and that of the bulk. The other is the lattice relaxation between the substrate and the film, defined as $\Delta a_s/a_s$, where a_s is the lattice constant of the substrate, and Δa_s is the difference between the lattice constant of the film and that of the substrate. For films thicker than a critical thickness, the epitaxial films may acquire lattice constants different from those of the substrates, thereby giving rise to extrinsic distortions such as dislocations, grain boundaries, and domains. On the other hand, lattice strain gives rise to more intrinsic distortion such as variation of the magnetic exchange and electron–phonon interactions. These two types of lattice distortion induced by three different substrates are listed in table 1 for the LCMO and LCCO films. We note that among the LCMO films, the lattice strain for the *a*- and *b*-axes is the largest in LCMO/STO, and the lattice relaxation is the largest in LCMO/YAO. On the other hand, for LCCO films, the lattice relaxation is only significant in LCCO/YAO.

The effects of lattice distortion on the resistivity and magnetoresistance of the LCMO

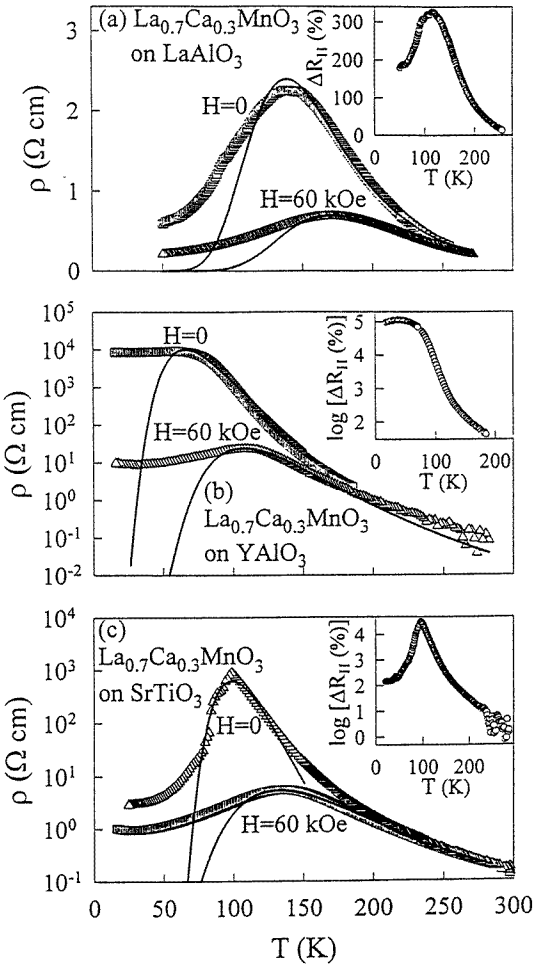

Figure 1. The effect of lattice distortion on the resistivity of $La_{0.7}Ca_{0.3}MnO_3$ epitaxial films on different substrates: (a) $LaAlO_3$, (b) $YAlO_3$, and (c) $SrTiO_3$. The solid lines are fitting curves obtained using equation (1), and the corresponding magnetoresistance (ΔR_H) versus temperature (T) data are shown in the insets.

films are illustrated in figures 1(a)–1(c), showing the highest zero-field resistivity, $\rho(H = 0, T)$, and the largest magnetoresistance, ΔR_H, at $H = 60$ kOe in the LCMO/YAO film which has the largest lattice relaxation. Here we define the magnetoresistance in a magnetic field H as $\Delta R_H \equiv [\rho(0) - \rho(H)]/\rho(H)$. Comparing the lattice distortion of LCMO/LAO and LCMO/STO, we note that the latter has a larger tensile strain, though smaller lattice relaxation. Our attribution of various substrate-dependent physical properties to the substrate-induced lattice distortion is further supported by our recent optical studies of the same LCMO films [17], showing distinct substrate-dependent frequency shifts (a few tens cm^{-1}) in the transverse optical phonon modes associated with the Mn–O–Mn bending ($\sim$330 cm^{-1}) and Mn–O stretching ($\sim$580 cm^{-1}) modes [17, 19]. The frequency shifts increase with the increasing lattice strain $\Delta a_0/a_0$ listed in table 1, and these unusually large frequency shifts with the lattice strain suggest strong electron–phonon coupling [19], and

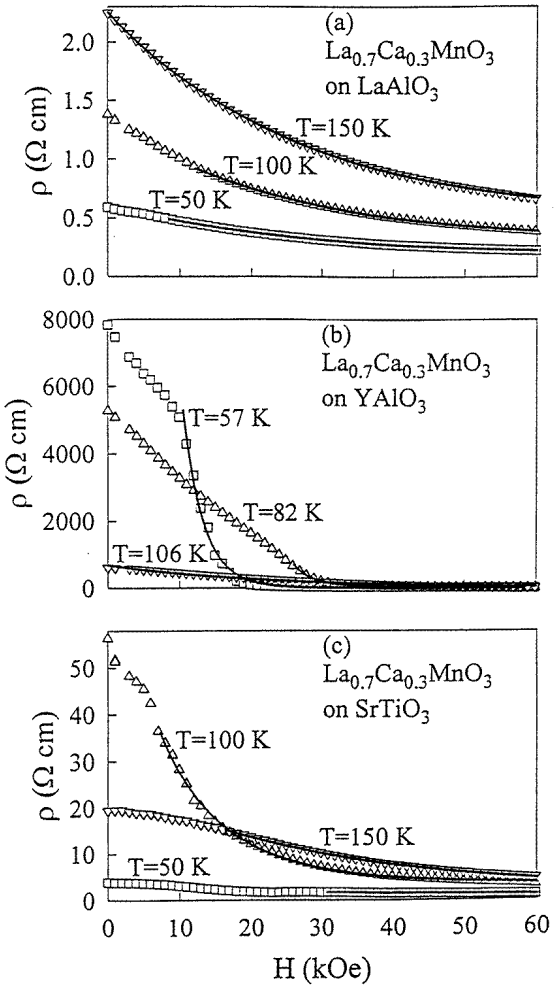

Figure 2. The magnetic field dependence of the resistivity (ρ versus H) at various constant temperatures for (a) LCMO/LAO, (b) LCMO/YAO, and (c) LCMO/STO epitaxial films. The solid lines are fitting curves obtained using equation (1) over the range of fields in which the expression is applicable.

are also supportive of the lattice polaron conduction scenario [2, 5]. We also note that for the least distorted films on the LAO substrate, the optical phonon frequencies are in good agreement with those in polycrystalline samples [19]. Furthermore, the linewidths of these optical phonon modes are found to be consistently narrower in thin films than those in polycrystalline samples.

In figures 2(a)–2(c), some representative resistivity data as functions of the magnetic field at various constant temperatures are shown for the annealed LCMO/LAO, LCMO/YAO, and LCMO/STO films. We note that the ρ–H isotherms are monotonically decreasing with H for all samples, and those for the least distorted films, of LCMO/LAO, are the smoothest. On the other hand, for both LCMO/STO and LCMO/YAO films, some isotherms exhibit a distinct change in the slope. We may consider the lattice polaron conduction mechanism [2, 5] which is important if the hopping rate of the itinerant electrons is sufficiently slow that it

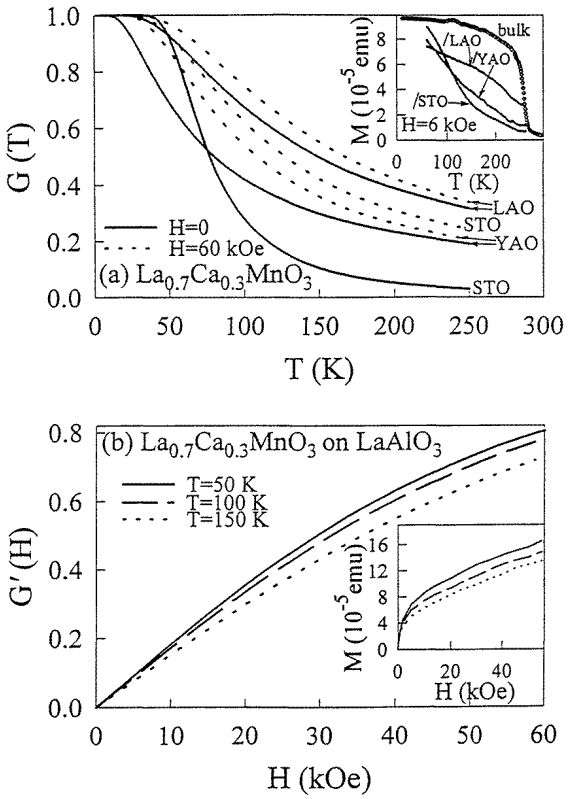

Figure 3. (a) The $G(T)$–T curves for LCMO/LAO, LCMO/STO, and LCMO/YAO films (the solid lines) at $H = 0$ and $H = 60$ kOe. The inset shows the temperature dependence of the magnetic moments $M(T)$ for LCMO/LAO, LCMO/STO, and LCMO/YAO films, and bulk LCMO, taken at $H = 6$ kOe. (b) The representative $G'(H)$–H isotherms for the LCMO/LAO film. The corresponding M–H data are shown in the inset.

is comparable to the optical phonon frequency. Assuming dominant polaron conduction at high temperatures ($T \sim T_C$), we obtain the fitting curves shown as the solid lines in figures 1 and 2 by using the following formulae which are obtained from the first-order polynomial approximations for the polaron conductivity [5, 20]:

$$\begin{aligned} \rho(T) &\approx \frac{\alpha T}{(1+G)} \exp\left[\frac{E_b(T)}{k_B T}\right] \equiv \frac{\alpha T}{(1+G)} \exp\left\{\frac{E_{b0}}{k_B T}\left[1 - G(T)\right]\right\} \\ \rho(H) &\approx \frac{\alpha T}{(1+G')} \exp\left[\frac{E_b(H)}{k_B T}\right] \equiv \frac{\alpha T}{(1+G')} \exp\left\{\frac{E_{b0}}{k_B T}\left[1 - G'(H)\right]\right\} \end{aligned} \tag{1}$$

where E_b is the polaron binding energy, α is a constant, and the unknown temperature and magnetic field dependences of E_b are approximated by, respectively, $G(T)$ and $G'(H)$ which satisfy the conditions imposed by the polaron model. That is, $E_b \to 0$ in the limit of complete magnetic order when the increasing hopping rate of the itinerant electrons exceeds the optical phonon frequency, and $E_b \to$ constant in the absence of long-range magnetic order. Thus, $0 \leqslant G, G' \leqslant 1$, and $G(T) \to 1$ for $T \ll T_C$, $G'(H) \to 1$ for large H. Furthermore, $G(T) \to 0$ for $T \to T_C$, and $G'(H) \to 0$ for $H \to 0$. Therefore $G(T)$ and $G'(H)$ are closely related to the normalized magnetization $m \equiv M/M_s$, with

M being the magnetization and M_s the saturation magnetization. Using equation (1) and the constraints given above, our best fit to the high-temperature ρ–T data (for T near to and above the resistive peak) and to the high-field ρ–H data (for H larger than where the 'kink' in the $\rho(H)$ curve appears) yields $G(T)$ and $G'(H)$ illustrated in figures 3(a) and 3(b), with the same parameter $E_{b0} \approx 0.35$ eV for all LCMO films on different substrates. On the other hand, at low temperatures the deviation of the resistivity data from the polaron model increases with the increasing substrate-induced lattice distortion, suggesting that the residual resistivity and magnetoresistance at low temperatures are largely determined by the lattice distortion.

A noteworthy correlation of the functions $G(T)$ and $G'(H)$ with the experimental magnetization data $M(T)$ and $M(H)$ is illustrated in figures 3(a) and 3(b). This correlation suggests the relevance of magnetic ordering to the electrical conduction, particularly for temperatures near T_C. The polaron binding energy ($E_{b0} \approx 0.35$ eV) derived from equation (1) compares favourably with the Jahn–Teller energy of $\sim$0.5 eV for undoped $LaMnO_3$ [2], and is much larger than that for the magnetic polarons due to the electron–spin interaction [21]. Although we caution that the exact forms of $G(T)$ and $G'(H)$ should not be taken literally, because the polaron model given in equation (1) is only an approximation and is limited to the high-temperature region, the analyses outlined above do provide a consistent picture of two types of contribution to the resistivity and magnetoresistance, with strong evidence of polaron hopping conduction at high temperatures, and a different scattering mechanism associated with the lattice distortion at low temperatures.

The low-temperature scattering mechanism may be understood by comparing the $M(T)$ data for all LCMO films and that for the bulk in figure 3(a). We note that the slower rise of magnetization below T_C for samples of larger lattice distortion, either intrinsic (strain) or extrinsic (relaxation), appears to be correlated with larger resistivity and magnetoresistance, suggesting increasing electron scattering induced by larger lattice distortion. One possible consequence of larger lattice distortion is a larger number of magnetic domains. Although all domains may undergo a ferromagnetic phase transition at the same T_C, the incompletely aligned moments of the magnetic domains due to either inhomogeneity or pinning by local defects below T_C give rise to more slowly rising magnetization and larger scattering of conduction electrons. Therefore an applied magnetic field has more significant effects on aligning the magnetic domains and reducing the resistivity in samples with larger lattice distortion.

As manifested in figure 1, the scenario of magnetic domain wall scattering is consistent with the larger resistivity and magnetoresistance at low temperatures where the polaron contribution becomes insignificant. Furthermore, the distinct change of slope in the low-temperature ρ–H isotherms of LCMO/STO and LCMO/YAO, samples with larger lattice distortion (see figure 2), also suggests better alignment of magnetic domains in higher fields. On the other hand, we find that the ρ–H isotherms of the least distorted films, of LCMO/LAO, can be consistently described by equation (1) over a large magnetic field range, indicating less significant magnetic domain wall scattering. The above conjecture is further confirmed by our studies of these samples using a scanning tunnelling microscope [18], showing the morphology of the sample surface to be well correlated with the magnetoresistance, with the larger magnetoresistance associated with the rougher surface induced by the larger lattice relaxation.

Having addressed the issue of lattice distortion effects on the magnetoresistance in the manganites, we proceed to investigate the necessity of lattice polaron conduction to the occurrence of CMR effects by studying the resistivity and magnetization of $La_{0.5}Ca_{0.5}CoO_3$ epitaxial films on LAO and YAO substrates. Despite comparable lattice relaxation and lattice

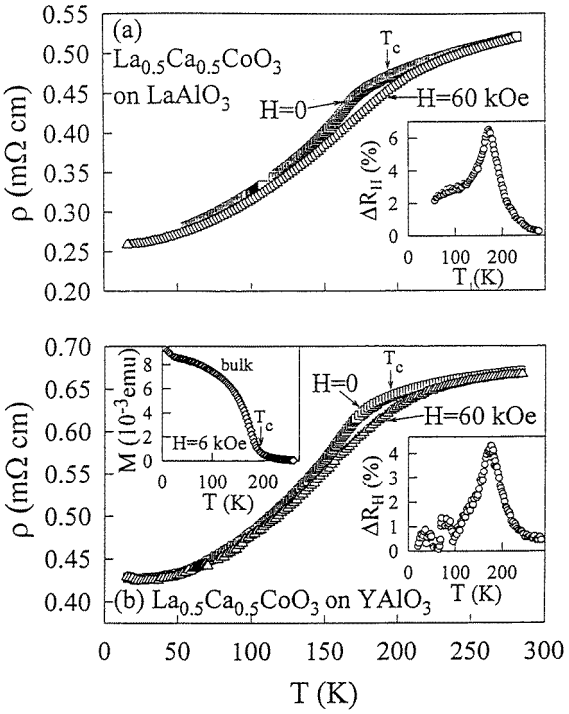

Figure 4. The effect of lattice distortion on the resistivity of $La_{0.5}Ca_{0.5}CoO_3$ epitaxial films on different substrates: (a) $LaAlO_3$; (b) $YAlO_3$. The corresponding magnetoresistance (ΔR_H) versus temperature (T) data as well as the M–T curve are shown in the insets.

strain in the manganites and in LCCO/YAO (see table 1), the magnitude and temperature dependence of the resistivity in the LCMO and LCCO systems exhibit sharp contrasts, as illustrated in figures 1(a)–1(c) and figures 4(a) and 4(b). Since the much higher electron mobility in the cobaltites tends to inhibit the formation of lattice polarons, the resistivity of the cobaltites may be understood in terms of the combination of conventional impurity, phonon, and disorder–spin scattering, with the disorder–spin scattering being the only magnetic field-dependent term. As shown in figure 4, for both LCCO/LAO and LCCO/YAO samples, the temperature below which a faster decrease in the zero-field resistivity occurs coincides with the Curie temperature $T_C \approx 180$ K, suggesting that magnetic ordering below T_C reduces the resistivity [15], and that the negative magnetoresistance near T_C is due to the field-induced suppression of spin fluctuations and of the corresponding scattering near T_C. Therefore the physical origin of the negative magnetoresistance in the cobaltites appears to be fundamentally different from that in the manganites, and the formation of lattice polarons seems to be essential for the occurrence of CMR effects in the manganites.

4. Conclusion

In summary, we have investigated the role of lattice distortion, polaron conduction, and Jahn–Teller coupling in the occurrence of the colossal negative magnetoresistance in perovskite oxides by comparing the electrical transport and magnetic properties of $La_{0.7}Ca_{0.3}MnO_3$ and $La_{0.5}Ca_{0.5}CoO_3$ films on substrates with different lattice constants.

The colossal negative magnetoresistance in LCMO films at high temperatures has been attributed to the conduction of lattice polarons, as manifested by a polaron binding energy of ∼0.35 eV, comparable to the Jahn–Teller energy, and by the resistivity being closely correlated with the magnetization. On the other hand, the low-temperature residual magnetoresistance in LCMO films is found to be correlated with the substrate-induced lattice distortion which yields excess magnetic domain wall scattering. In contrast, much smaller magnetoresistance is observed in LCCO films, with lattice distortion comparable to that of LCMO films, indicating that lattice distortion alone is insufficient to yield colossal negative magnetoresistance. We therefore conclude that the formation of lattice polarons due to the strong electron–phonon coupling and the Jahn–Teller effect in the manganites appears essential for the occurrence of CMR effects, and that lattice distortion further enhances the magnitude of the negative magnetoresistance.

Acknowledgments

The research at Caltech is supported by the Packard Foundation and the National Aeronautics and Space Administration (NASA). Part of the research was performed by the Center for Space Microelectronics Technology, Jet Propulsion Laboratory, Caltech, under a contract with NASA. We thank Nikko Hitech International Incorporated for supplying the $YAlO_3$ substrates used in this work.

References

[1] von Helmolt R, Wecker J, Holzapfel, Schultz L and Samwer K 1993 *Phys. Rev. Lett.* **71** 2331
Jin S, Tiefel T H, McCormack M, Fastnacht R A, Ramesh R and Chen L H 1994 *Science* **264** 413
[2] Millis A J, Littlewood P B and Shraiman B I 1995 *Phys. Rev. Lett.* **74** 5144
Millis A J, Shraiman B I and Mueller R 1996 *Phys. Rev. Lett.* **77** 175
[3] Jin S, O'bryan H M, Tiefel T H, McCormack M and Rhodes W W 1995 *Appl. Phys. Lett.* **66** 382
Jin S, Tiefel T H, McCormack M, O'bryan H M, Chen L H, Ramesh R and Schurig D 1995 *Appl. Phys. Lett.* **67** 557
[4] Hwang H Y, Cheong S W, Radaelli P G, Marezio M and Batlogg B 1995 *Phys. Rev. Lett.* **75** 914
[5] Jia Y X, Lu L, Khazeni K, Crespi V H, Zettl A and Cohen M L 1995 *Phys. Rev.* B **52** 9147
[6] Khazeni K, Jia Y X, Lu L, Crespi V H, Cohen M L and Zettl A 1996 *Phys. Rev. Lett.* **76** 295
[7] Ibarra M R, Algarabel P A, Marquina C, Blasco J and Garcia J 1995 *Phys. Rev. Lett.* **75** 3541
[8] Zhao G-M, Conder K, Keller H and Muller K A 1996 *Nature* **381** 676
[9] Jonker G H and van Santen J H 1950 *Physica* **16** 337
van Santen J H and Jonker G H 1950 *Physica* **16** 599
[10] Zener C 1951 *Phys. Rev.* **82** 403
[11] Wollan E O and Koehler W C 1955 *Phys. Rev.* **100** 545
[12] Goodenough J B, Wold A, Arnott R J and Menyuk N 1961 *Phys. Rev.* **124** 373
Goodenough J B 1971 *Progress in Solid State Chemistry* vol 5, ed H Reiss (Oxford: Pergamon)
[13] de Gennes P G 1960 *Phys. Rev.* **118** 141
[14] Ohbayashi H, Kudo T and Gejo T 1974 *Japan. J. Appl. Phys.* **13** 1
[15] Mahendiran R, Raychaudhuri A K, Chainani A and Sarma D D 1995 *J. Phys.: Condens. Matter* **7** L561
Yamaguchi S, Taniguchi H, Takagi H, Arima T and Tokura Y 1995 *J. Phys. Soc. Japan* **64** 1885
[16] Vasquez R P 1996 *Phys. Rev.* B **54** 14 938
[17] Boris A V, Bazhenov A V, Kovaleva N N, Samoilov A V, Yeh N-C and Vasquez R P 1997 *J. Appl. Phys.* **81** at press
[18] Yeh N-C, Fu C-C, Wei J Y T, Vasquez R P, Huynh J and Beach G 1997 *J. Appl. Phys.* **81** at press
[19] Kim K H, Gu J Y, Choi H S, Park G W and Noh T W 1996 *Phys. Rev. Lett.* **77** 1877
[20] Mott N F and Davis E A 1979 *Electronic Processes in Non-crystalline Materials* (Oxford: Clarendon)
[21] Kusters R M, Singleton J, Keen D A, McGreevy R, and Hayes W 1989 *Physica* B **155** 362
[22] Taguchi H, Shimada M and Koizumi M 1982 *J. Solid State Chem.* **41** 329